

# Antioxidant activity of modified 2,6-Di-*tert*-butylphenols with pyridine moiety

## Abstract

A series of 2,6-di-*tert*-butylphenols with pyridine moiety and their hydrophilic forms were synthesized and characterized by NMR, IR, X-ray and elemental analysis. The redox properties of compounds were studied by cyclic voltammetry (CV). Chemical oxidation of compounds under investigation leading to relatively stable radicals was studied by EPR. Antioxidant activity was evaluated in model reactions of hydrogen atom abstraction (DPPH-test) and one-electron reduction (CUPRAC-test). It was shown that modified 2,6-di-*tert*-butylphenols possess radical scavenging activity of prolonged action, achieving its maximum on 20 h time spans. The antioxidant properties *in vitro* in oxidation of linoleic acid by *lipoxygenase*, in reaction with superoxide radical-anion generated from xanthine/xanthine-oxidase enzymatic system, and in induced lipid peroxidation of rat liver homogenates were studied. The study of lipid peroxidation demonstrated high antioxidant activity for both lipophilic and hydrophilic compounds. The "structure-activity" analysis shows that the length of the linker between functional groups and position of substituent in pyridine cycle affects the antioxidant activity. Results of this study open the scopes for the search of novel water-soluble cyto-, neuroprotectors and physiologically active compounds with antioxidant mode of action.

**Keywords:** 2,6-di-*tert*-butylphenol, pyridines, antioxidants, X-ray analysis, DPPH, ROS, radical scavenging activity, electrochemistry, EPR, lipid peroxidation

Volume 8 Issue 3 - 2020

Evgeny A Nikitin,<sup>1</sup> Dmitry B Shpakovsky,<sup>1</sup> Alexey D Pryakhin,<sup>1</sup> Taisiya A Antonenko,<sup>1</sup> Vladimir Yu Tyurin,<sup>1</sup> Anna A Kazak,<sup>1</sup> Alexander N Ulyanov,<sup>1</sup> Viktor A Tafeenko,<sup>1</sup> Leonid A Aslanov,<sup>1</sup> Ludmila G Dubova,<sup>2</sup> Elena A Lysova,<sup>2</sup> Elena F Shevtsova,<sup>2</sup> Elena R Milaeva<sup>1,2</sup>

<sup>1</sup>Department of Chemistry, Lomonosov Moscow State University, Russia

<sup>2</sup>Institute of Physiologically Active Compounds of RAS, Russia

**Correspondence:** Elena R Milaeva, Department of Chemistry, Lomonosov Moscow State University, 119991, Moscow, Leninskie gory, 1-3, Russia, Email milaeva@med.chem.msu.ru

Received: April 24, 2020 | Published: May 11, 2020

## Introduction

Oxidative stress is an imbalance between the action of antioxidants and pro-oxidants in favor of the latter.<sup>1,2</sup> Pro-oxidants are generated in some cellular processes, including aerobic metabolism. Under certain conditions, pro-oxidants are produced at increased rate, thus violating the balance. Reactive oxygen species (ROS) such as superoxide radical-anion O<sub>2</sub><sup>-</sup>, hydroxyl radical HO<sup>•</sup>, hydrogen peroxide H<sub>2</sub>O<sub>2</sub>, lipid hydroperoxides and peroxy radicals are among the most well-known oxygen metabolites. ROS cause damage of intracellular structures such as proteins, nucleic acids, lipids, membranes by initializing destructive chain radical processes.<sup>3</sup> It is well known that oxidative stress participates in a pathogenesis of many diseases, e.g. ischemia, atherosclerosis, inflammation,<sup>4</sup> schizophrenia,<sup>5</sup> pre-eclampsia,<sup>6</sup> epilepsy,<sup>7</sup> psoriasis,<sup>8</sup> various types of cancer.<sup>9,10</sup> Moreover, there exists the radical theory of ageing<sup>11,12</sup> which assumes that endogenously produced ROS cause cumulative damage of living tissues due to disability of the organism to be entirely protected from active radicals. Considering this, the search of new methods of preventing such pathologies is a task of a great importance.

Antioxidants are the compounds which can neutralize the negative effect of the oxidative stress. They can be divided into several groups according to the mechanism of their action: first and the largest one includes substances that scavenge active radicals thus inhibiting chain radical processes; next group suppresses or prevents the formation of pro-oxidants; the last one repairs the damage caused by active particles.<sup>13</sup> Living organism possesses complex antioxidant defense system which prevents cellular damage and regulates the toxic impact caused by ROS.<sup>14</sup> It consists of low-molecular non-enzymatic natural antioxidants (e.g. ascorbic acid, tocopherols, lipoic acid, and carotenoids, etc.) and of enzymatic antioxidants such as

superoxide dismutase (SOD), catalase, glutathione and glutathione dependent enzymes as well. These compounds demonstrate different mechanisms of activity: a dismutation of superoxide radical-anion by SOD, scavenging of hydroxyl radical HO<sup>•</sup>, interaction either with peroxy radicals of lipids or lipid hydroperoxides breaking down the chain radical processes of lipid peroxidation.<sup>15</sup> Thus, these natural antioxidants act in accordance with their chemical reactivity providing the non-harmful products.

Phenol derivatives (e.g. tocopherols, tyrosine, thyroxine, etc.) involved in radical biochemical processes are essential for cellular homeostasis. 2,6-Di-alkylphenols are less toxic than their unsubstituted analogues and often used as antioxidants, radical scavengers and biomimetics of  $\alpha$ -tocopherol. The mechanism of their action includes formation of stable phenoxyl radicals and inhibition of further radical chain reactions.<sup>16</sup> In last decade we focused on the synthesis of functionalized 2,6-di-*tert*-butylphenols and their metal complexes. An approach to combine antioxidant fragment with different metals in one molecule seems promising. Metalloporphyrins with 2,6-di-*tert*-butylphenol groups demonstrated dependence of the antioxidant properties on the nature of the metal.<sup>17</sup> This provides multiple advantages: chemical structure and chemical properties may easily be altered by changing of metal, intermolecular redox process stabilizes phenoxyl radicals and terminal group can be introduced in order to endow the molecule with special properties, e.g. hydro/lipophilicity or affinity. Such compounds demonstrated wide spectrum of properties including antioxidant<sup>18-21</sup> radical scavenging<sup>22,23</sup> and cytotoxic properties<sup>24,25</sup> that lets one to consider them as promising drug candidates.<sup>26,27</sup>

The goal of this study was the synthesis and evaluation of antioxidant activity of hybrid compounds containing both antioxidant

moiety and coordination group capable to bind metal ions. A series of new pyridine derivatives containing 2,6-di-*tert*-butylphenol fragments (Scheme 1) was synthesized and characterized by physicochemical methods. Redox and antioxidant properties of compounds were evaluated by cyclic voltammetry and in model reactions with stable 2,2-diphenyl-1-picrylhydrazyl radical (DPPH), CUPRAC-test, enzymatic reactions of *lipoxygenase* (LOX 1-B) and *xanthine oxidase*. Additionally, compounds were studied in lipid peroxidation of rat liver homogenates *ex vivo*.

## Materials and methods

2,6-di-*tert*-butylphenol (99%), 3,5-di-*tert*-butyl-4-hydroxybenzoic acid (98%), triethylamine ( $\geq 99\%$ ), 2-picolyamine (99%), 3-picolyamine ( $\geq 99\%$ ) and 4-picolyamine (98%) were provided by Sigma-Aldrich and used with no further purification. 3-(3,5-di-*tert*-butyl-4-hydroxyphenyl)propionic acid.<sup>28</sup> The solvents (EtOH (95%),  $\text{CHCl}_3$ ,  $\text{CH}_2\text{Cl}_2$ , MeOH, Et<sub>2</sub>O, toluene, acetone, and petroleum ether (b.p. 40–70°C)) were used as-received.

Chlorides of 3,5-di-*tert*-butyl-4-hydroxybenzoic acid and 3-(3,5-di-*tert*-butyl-4-hydroxyphenyl)propionic acid were synthesized by reflux of acids with (10 eqv.) thionyl chloride in petroleum ether for 1 h followed by the removal of solvent *in vacuo*.

The NMR spectra were measured on a Bruker AMX-400 spectrometer in  $\text{CDCl}_3$  and DMSO-*d*<sub>6</sub> (<sup>1</sup>H, 400 MHz; <sup>13</sup>C, 100.6 MHz). The IR spectra were recorded on an IR200 Fourier-transform IR spectrophotometer (Thermo Nicolet) as KBr pellets. EPR spectra were recorded with a Bruker EMX spectrometer at the X-band range (9.8 GHz). The measurements were carried out after pre-evacuation of samples solutions (concentration 0.1 mM). The oxidant PbO<sub>2</sub> was taken in a tenfold excess.

## General synthesis of substituted amides (1–6) and their hydrochlorides (1a–6a)

A mixture of NEt<sub>3</sub> (77  $\mu\text{l}$ , 0.55 mmol) and corresponding picolyamine (52  $\mu\text{l}$ , 0.5 mmol) in degassed  $\text{CH}_2\text{Cl}_2$  (1 ml) was added dropwise to a solution of 3,5-di-*tert*-butyl-4-hydroxybenzoic acid chloride (137 mg, 0.5 mmol) or 3-(3,5-di-*tert*-butyl-4-hydroxyphenyl)propionic acid chloride (148 mg, 0.5 mmol) in degassed  $\text{CH}_2\text{Cl}_2$  (20 ml) and reaction mixture was stirred for 24 h. Solvent was removed *in vacuo*, residue was washed by petroleum ether (3x5 ml) and H<sub>2</sub>O (3x5 ml) and dried in the air.

### 3,5-di-*tert*-butyl-4-hydroxy-N-(pyridine-2-yl-methyl)benzamide (1)

Compound **1** was recrystallized from  $\text{CH}_2\text{Cl}_2$ -petroleum ether to give 133 mg of colorless powder (78%). Mp 170–172°C. IR,  $\text{cm}^{-1}$ : 3345.9 ( $\nu$  O-H bound); 3332.5 ( $\nu$  N-H); 2873.4–2966.0 ( $\nu$  C-H); 1633.4 ( $\nu$  C=O); 1523.5; 1434.8; 1322.9; 1234.2; 757.9. <sup>1</sup>H NMR (400 MHz,  $\text{CDCl}_3$ ,  $\delta$ , ppm): 1.41 (s, 18H, 2 Bu<sup>t</sup>); 4.55 (d, 2H, CH<sub>2</sub>, <sup>3</sup>J<sub>HH</sub>=6 Hz); 7.25 (dd, 1H, H-Py, <sup>3</sup>J<sub>HH</sub>=5 Hz, <sup>3</sup>J<sub>HH</sub>=4 Hz); 7.30 (d, 1H, H-Py, <sup>3</sup>J<sub>HH</sub>=4 Hz); 7.70 (s, 2H, H-Ar); 7.74 (dd, 1H, H-Py, <sup>3</sup>J<sub>HH</sub>=4 Hz, <sup>3</sup>J<sub>HH</sub>=5 Hz); 8.50 (d, 1H, H-Py, <sup>3</sup>J<sub>HH</sub>=4 Hz); 8.96 (t, 1H, NH, <sup>3</sup>J<sub>HH</sub>=6 Hz). <sup>13</sup>C NMR (100.6 MHz,  $\text{CDCl}_3$ ,  $\delta$ , ppm): 30.66 (C(CH<sub>3</sub>)<sub>3</sub>); 35.07 (C(CH<sub>3</sub>)<sub>3</sub>); 45.16 (NHCH<sub>2</sub>Py); 121.38 (C Py); 122.42 (C Py); 124.62 (C2 Ar); 125.69 (C1 Ar); 137.11 (C Py); 138.71 (C3 Ar); 149.19 (C Py); 157.28 (C4 Ar); 159.77 (C Py); 167.40 (C=O). Elemental analysis, calcd for C<sub>21</sub>H<sub>28</sub>N<sub>2</sub>O<sub>2</sub> (%): C, 74.08; H, 8.29; N, 8.23. Found (%): C, 73.89; H, 8.60; N, 8.49.

### 3,5-di-*tert*-butyl-4-hydroxy-N-(pyridine-3-yl-methyl)benzamide (2)

Compound **2** was recrystallized from  $\text{CH}_2\text{Cl}_2$ -petroleum ether to give 153 mg of colorless powder (90%). Mp 108–110°C. IR,  $\text{cm}^{-1}$ : 3627.5 ( $\nu$  O-H free); 3224.4 ( $\nu$  N-H); 3060.5–2867.6 ( $\nu$  C-H); 1629.6 ( $\nu$  C=O); 1598.7; 1546.6; 1430.9; 1363.4; 1326.8; 1224.6; 711.6. <sup>1</sup>H NMR (400 MHz,  $\text{CDCl}_3$ ,  $\delta$ , ppm): 1.46 (s, 18H, 2 Bu<sup>t</sup>); 4.67 (d, 2H, CH<sub>2</sub>, <sup>3</sup>J<sub>HH</sub>=6 Hz); 5.62 (s, 1H, OH); 6.70 (t, 1H, NH, <sup>3</sup>J<sub>HH</sub>=6 Hz); 7.27 (dd, 1H, H-Py, <sup>3</sup>J<sub>HH</sub>=6 Hz, <sup>3</sup>J<sub>HH</sub>=8 Hz); 7.65 (s, 2H, H-Ar); 7.73 (d, 1H, H-Py, <sup>3</sup>J<sub>HH</sub>=8 Hz); 8.53 (d, 1H, H-Py, <sup>3</sup>J<sub>HH</sub>=6 Hz); 8.59 (s, 1H, H-Py). <sup>13</sup>C NMR (100.6 MHz,  $\text{CDCl}_3$ ,  $\delta$ , ppm): 30.12 (C(CH<sub>3</sub>)<sub>3</sub>); 34.42 (C(CH<sub>3</sub>)<sub>3</sub>); 41.39 (CONHCH<sub>2</sub>Py); 123.62 (C Py); 124.23 (C2-Ar); 125.05 (C1-Ar); 134.51 (C Py); 135.78 (C Py); 136.02 (C3-Ar); 148.79 (C Py); 149.18 (C Py); 157.07 (C4-Ar); 168.21 (C=O). Elemental analysis, calcd for C<sub>21</sub>H<sub>28</sub>N<sub>2</sub>O<sub>2</sub> (%): C, 74.08; H, 8.29; N, 8.23; Found (%): C, 74.04; H, 7.97; N, 8.18;

### 3,5-di-*tert*-butyl-4-hydroxy-N-(pyridine-4-yl-methyl)benzamide (3)

Compound **3** was recrystallized from  $\text{CH}_2\text{Cl}_2$ -petroleum ether to give 147 mg of colorless powder (86%). Mp 210–213°C. IR,  $\text{cm}^{-1}$ : 3667.9 ( $\nu$  O-H free); 3232.1 ( $\nu$  N-H); 3064.3–2875.3 ( $\nu$  C-H); 1631.5 ( $\nu$  C=O); 1602.6; 1540.8; 1425.1; 1373.1; 1321.0; 1257.4; 1097.3; 740.5. <sup>1</sup>H NMR (400 MHz, DMSO-*d*<sub>6</sub>,  $\delta$ , ppm): 1.41 (s, 18H, 2 Bu<sup>t</sup>); 4.47 (d, 2H, CH<sub>2</sub>, <sup>3</sup>J<sub>HH</sub>=6 Hz); 7.29 (d, 2H, H-Py, <sup>3</sup>J<sub>HH</sub>=6 Hz); 7.45 (s, 1H, OH); 7.69 (s, 2H, H-Ar); 8.50 (d, 2H, H-Py, <sup>3</sup>J<sub>HH</sub>=6 Hz); 8.94 (t, 1H, NH, <sup>3</sup>J<sub>HH</sub>=6 Hz). <sup>13</sup>C NMR (100.6 MHz, DMSO-*d*<sub>6</sub>,  $\delta$ , ppm): 30.65 (C(CH<sub>3</sub>)<sub>3</sub>); 35.07 (C(CH<sub>3</sub>)<sub>3</sub>); 42.18 (CONHCH<sub>2</sub>Py); 122.61 (C Py); 124.61 (C2-Ar); 125.48 (C1-Ar); 138.74 (C3-Ar); 149.56 (C Py); 149.94 (C Py); 157.37 (C4-Ar); 167.48 (C=O). Elemental analysis, calcd for C<sub>21</sub>H<sub>28</sub>N<sub>2</sub>O<sub>2</sub>·0.5 H<sub>2</sub>O (%): C, 72.17; H, 8.36; N, 8.02. Found (%): C, 71.87; H, 8.02; N, 8.15.

### 3-(3,5-di-*tert*-butyl-4-hydroxyphenyl)-N-(pyridine-2-yl-methyl)propanamide (4)

Compound **4** was recrystallized from  $\text{CH}_2\text{Cl}_2$ -petroleum ether to give 83 mg of colorless crystals (45%). Mp 127–130°C. IR,  $\text{cm}^{-1}$ : 3100–3270 ( $\nu$  O-H bound,  $\nu$  N-H); 3036.9–2866.7 ( $\nu$  C-H); 1633.4 ( $\nu$  C=O); 1544.2; 1478.6; 1439.6; 1360.1; 1197.1; 1156.1; 878.4; 771.4; 749.7. <sup>1</sup>H NMR (400 MHz,  $\text{CDCl}_3$ ,  $\delta$ , ppm): 1.43 (s, 18H, 2 Bu<sup>t</sup>); 2.59 (t, 2H, CH<sub>2</sub>, <sup>3</sup>J<sub>HH</sub>=8 Hz); 2.95 (t, 2H, CH<sub>2</sub>, <sup>3</sup>J<sub>HH</sub>=8 Hz); 4.59 (d, 2H, CH<sub>2</sub>, <sup>3</sup>J<sub>HH</sub>=5 Hz); 5.09 (s, 1H, OH); 6.71 (br. s, 1H, NH); 7.04 (s, 2H, H-Ar); 7.19–7.22 (m, 2H, 2 H-Py); 7.64–7.69 (m, 1H, H-Py); 8.54 (d, 1H, H-Py, <sup>3</sup>J<sub>HH</sub>=5 Hz). NMR <sup>13</sup>C (100.6 MHz,  $\text{CDCl}_3$ ,  $\delta$ , ppm): 33.23 (C(CH<sub>3</sub>)<sub>3</sub>); 34.70 (ArCH<sub>2</sub>CH<sub>2</sub>CO); 37.22 (C(CH<sub>3</sub>)<sub>3</sub>); 41.91 (ArCH<sub>2</sub>CH<sub>2</sub>CO); 47.39 (CONHCH<sub>2</sub>Py); 124.99 (C2-Ar); 125.25 (C1-Ar); 127.75 (C Py); 132.74 (C Py); 134.35 (C Py); 138.86 (C3-Ar); 139.70 (C Py); 151.89 (C Py); 159.30 (C4-Ar); 175.44 (C=O). Elemental analysis, calcd for C<sub>23</sub>H<sub>32</sub>N<sub>2</sub>O<sub>2</sub> (%): C, 74.96; H, 8.75; N, 7.60; Found (%): C, 75.37; H, 8.89; N, 7.43.

### 3-(3,5-di-*tert*-butyl-4-hydroxyphenyl)-N-(pyridine-3-yl-methyl)propanamide (5)

Compound **5** was recrystallized from  $\text{CH}_2\text{Cl}_2$ -petroleum ether to give 140 mg of colorless crystals (76%). Mp 145–147°C. IR,  $\text{cm}^{-1}$ : 3565.7 ( $\nu$  O-H bound); 3249.5 ( $\nu$  N-H); 3075.9–2867.6 ( $\nu$  C-H); 1643.1 ( $\nu$  C=O); 1556.3; 1483.0; 1429.0; 1359.6; 1268.9 1238.1; 1101.2; 1039.4; 887.1; 869.7; 752.1; 719.3. <sup>1</sup>H NMR (400 MHz,  $\text{CDCl}_3$ ,  $\delta$ , ppm): 1.43 (s, 18H, 2 Bu<sup>t</sup>); 2.54 (t, 2H, CH<sub>2</sub>, <sup>3</sup>J<sub>HH</sub>=8 Hz);

2.93 (t, 2H, CH<sub>2</sub>, <sup>3</sup>J<sub>HH</sub>=8 Hz); 4.45 (d, 2H, CH<sub>2</sub>, <sup>3</sup>J<sub>HH</sub>=6 Hz); 5.17 (s, 1H, OH); 5.99 (t, 1H, NH, <sup>3</sup>J<sub>HH</sub>=6 Hz); 7.01 (s, 2H, H-Ar); 7.24 (dd, 1H, H-Py, <sup>3</sup>J<sub>HH</sub>=8 Hz, <sup>3</sup>J<sub>HH</sub>=4 Hz); 7.49 (d, 1H, H-Py, <sup>3</sup>J<sub>HH</sub>=8 Hz); 8.45 (d, 1H, H-Py, <sup>3</sup>J<sub>HH</sub>=4 Hz); 8.49 (s, 1H, H-Py). NMR <sup>13</sup>C (100.6 MHz, CDCl<sub>3</sub>, δ, ppm): 30.32 (C(CH<sub>3</sub>)<sub>3</sub>); 31.69 (ArCH<sub>2</sub>CH<sub>2</sub>CO); 34.32 (C(CH<sub>3</sub>)<sub>3</sub>); 38.92 (ArCH<sub>2</sub>CH<sub>2</sub>CO); 40.95 (CONHCH<sub>2</sub>Py); 123.65 (C1-Ar); 124.84 (C2-Ar); 131.14 (C Py); 135.54 (C Py); 136.14 (C3-Ar); 148.39 (C Py); 148.83 (C Py); 149.07 (C Py); 152.26 (C4-Ar); 175.44 (C=O). Elemental analysis, calcd for C<sub>23</sub>H<sub>32</sub>N<sub>2</sub>O<sub>2</sub> (%): C, 74.96; H, 8.75; N, 7.60. Found (%): C, 75.12; H, 9.02; N, 7.84.

### 3-(3,5-di-tert-butyl-4-hydroxyphenyl)-N-(pyridine-4-yl-methyl)propanamide (6)

Compound **6** was recrystallized from CH<sub>2</sub>Cl<sub>2</sub>-petroleum ether to give 144 mg of colorless crystals (78%). Mp 163-165°C. IR, cm<sup>-1</sup>: 3253.8-3205.6 (ν O-H bound, ν N-H); 3070.6-2871.0 (ν C-H); 1636.8 (ν C=O); 1606.9; 1562.5; 1431.4; 1417.9; 1359.6; 1235.7; 1219.8; 1167.2; 1110.8; 1067.9; 1000.4; 885.2; 870.2; 793.6; 753.6; 697.6. <sup>1</sup>H NMR (400 MHz, CDCl<sub>3</sub>, δ, ppm): 1.43 (s, 18H, 2 Bu<sup>t</sup>); 2.59 (t, 2H, CH<sub>2</sub>, <sup>3</sup>J<sub>HH</sub>=8 Hz); 2.95 (t, 2H, CH<sub>2</sub>, <sup>3</sup>J<sub>HH</sub>=8 Hz); 4.45 (d, 2H, CH<sub>2</sub>, <sup>3</sup>J<sub>HH</sub>=6 Hz); 5.16 (s, 1H, OH); 5.85 (t, 1H, NH, <sup>3</sup>J<sub>HH</sub>=6 Hz); 7.02 (d, 2H, CH-Py, <sup>3</sup>J<sub>HH</sub>=6 Hz); 7.03 (s, 2H, H-Ar); 8.50 (d, 2H, H-Py, <sup>3</sup>J<sub>HH</sub>=6 Hz). NMR <sup>13</sup>C (100.6 MHz, CDCl<sub>3</sub>, δ, ppm): 30.32 (C(CH<sub>3</sub>)<sub>3</sub>); 31.66 (ArCH<sub>2</sub>CH<sub>2</sub>CO); 34.34 (C(CH<sub>3</sub>)<sub>3</sub>); 38.80 (ArCH<sub>2</sub>CH<sub>2</sub>CO); 45.16 (CONHCH<sub>2</sub>Py); 122.10 (C Py); 124.88 (C2-Ar); 131.00 (C1-Ar); 136.12 (C3-Ar); 147.41 (C Py); 149.98 (C Py); 152.31 (C4-Ar); 172.59 (C=O). Elemental analysis, for C<sub>23</sub>H<sub>32</sub>N<sub>2</sub>O<sub>2</sub> calcd (%): C, 74.96; H, 8.75; N, 7.60. Found (%): C, 74.18; H, 8.78; N, 7.83.

### General synthesis of hydrochlorides (1a-6a)

To a corresponding amide (0.1 mmol) in methanol (2 ml), conc. HCl (35%, 17 μl, 0.2 mmol) was added and stirred for 5 min. Then toluene (2 ml) was added with stirring for 5 min more. Solvents were removed *in vacuo* and then toluene (1 ml), methanol (1 ml) and chloroform (1 ml) were successively added and removed *in vacuo*. This operation was repeated twice, yield was quantitative.

### 3,5-di-tert-butyl-4-hydroxy-N-(pyridine-2-yl-methyl)benzamide hydrochloride (1a)

37 mg (100%) of yellowish powder of compound **1a** was obtained. Mp 185-190°C. IR, cm<sup>-1</sup>: 3628.4 (ν O-H free); 3388.6 (ν N-H); 3062.9-2874.4 (ν C-H); 1622.3 (ν C=O); 1539.9; 1470.0; 1434.3; 1364.9; 1317.1; 1241.0 1161.9; 1121.9; 768.0. NMR <sup>1</sup>H, (400 MHz, CDCl<sub>3</sub>, δ, ppm): 1.47 (s, 18H, 2 Bu<sup>t</sup>); 5.04 (br.s, 2H, CH<sub>2</sub>); 5.62 (s, 1H, OH); 7.85 (s, 2H, Ar); 8.09 (br.s, 1H, Py); 8.37 (br.s, 1H, Py); 8.66 (br.s, 1H, Py); 8.87 (br.s, 1H, Py). NMR <sup>13</sup>C (100.6 MHz, CDCl<sub>3</sub>, δ, ppm): 30.27 (C(CH<sub>3</sub>)<sub>3</sub>); 34.50 (C(CH<sub>3</sub>)<sub>3</sub>); 41.31 (CONHCH<sub>2</sub>Py); 123.29 (C Py); 125.14 (C2-Ar); 125.37 (C1-Ar); 127.94 (C Py); 135.95 (C3-Ar); 141.12 (C Py); 145.83 (C Py); 154.56 (C Py); 157.55 (C4-Ar); 168.13 (C=O). Elemental analysis, calcd for C<sub>21</sub>H<sub>28</sub>N<sub>2</sub>O<sub>2</sub>·HCl (%): C, 66.92; H, 7.75; N, 7.43. Found (%): C, 66.70; H, 7.11; N, 7.05.

### 3,5-di-tert-butyl-4-hydroxy-N-(pyridine-3-yl-methyl)benzamide hydrochloride (2a)

37 mg (100%) of colorless powder of compound **2a** was obtained. Mp 198-201°C. IR, cm<sup>-1</sup>: 3623.6 (ν O-H free); 3216.7 (ν N-H); 3055.7-2877.8 (ν C-H); 1629.6 (ν C=O); 1600.2; 1537.0; 1465.2; 1432.9; 1329.7; 1255.9; 1235.2; 1030.8; 888.1; 753.1; 681.7. NMR

<sup>1</sup>H, (400 MHz, DMSO-d<sub>6</sub>, δ, ppm): 1.38 (s, 18H, 2 Bu<sup>t</sup>); 4.60 (s, 2H, CH<sub>2</sub>); 7.67 (s, 2H, Ar); 8.00 (dd, 1H, Py, <sup>3</sup>J<sub>HH</sub>=6 Hz); 8.50 (d, 1H, Py, <sup>3</sup>J<sub>HH</sub>=8 Hz); 8.81 (d, 1H, Py, <sup>3</sup>J<sub>HH</sub>=6 Hz); 8.87 (s, 1H, Py). NMR <sup>13</sup>C (100.6 MHz, DMSO-d<sub>6</sub>, δ, ppm): 30.21 (C(CH<sub>3</sub>)<sub>3</sub>); 34.64 (C(CH<sub>3</sub>)<sub>3</sub>); 45.26 (CONHCH<sub>2</sub>Py); 124.31 (C2-Ar); 124.53 (C1-Ar); 126.87 (C Py); 138.35 (C3-Ar); 140.06 (C Py); 140.37 (C Py); 140.72 (C Py); 144.46 (C Py); 156.99 (C4-Ar); 167.11 (C=O). Elemental analysis, calcd for C<sub>21</sub>H<sub>28</sub>N<sub>2</sub>O<sub>2</sub>·HCl (%): C, 66.92; H, 7.75; N, 7.43. Found (%): C, 66.61; H, 7.01; N, 7.52.

### 3,5-di-tert-butyl-4-hydroxy-N-(pyridine-4-yl-methyl)benzamide hydrochloride (3a)

37 mg (100%) of yellowish powder of compound **3a** was obtained. Mp 260-263°C. IR, cm<sup>-1</sup>: 3388.8-3233.6 (ν O-H bound; ν N-H); 3059.0-2872.5 (ν C-H); 1631.5 (ν C=O); 1604.0; 1544.2; 1473.8; 1427.6; 1321.5; 1298.8; 1257.4; 1095.9; 905.9; 739.1. NMR <sup>1</sup>H, (400 MHz, CDCl<sub>3</sub>, δ, ppm): 1.40 (s, 18H, CH<sub>3</sub>); 4.81 (br.s, 2H, CH<sub>2</sub>); 5.65 (s, 1H, OH); 7.81 (s, 2H, Ph); 7.93 (br.s, 2H, Py); 8.56 (br.s, 2H, Py); 8.84 (br.s, 1H, NH). NMR <sup>13</sup>C (100.6 MHz, CDCl<sub>3</sub>, δ, ppm): 29.81 (C(CH<sub>3</sub>)<sub>3</sub>); 34.07 (C(CH<sub>3</sub>)<sub>3</sub>); 45.53 (CONHCH<sub>2</sub>Py); 123.36 (C Py); 124.64 (C2-Ar); 125.37 (C1-Ar); 135.69 (C Py); 139.82 (C3-Ar); 157.08 (C Py); 161.43 (C4-Ar); 168.21 (C=O). Elemental analysis, calcd for C<sub>21</sub>H<sub>28</sub>N<sub>2</sub>O<sub>2</sub>·HCl (%): C, 66.92; H, 7.75; N, 7.43. Found (%): C, 66.02; H, 7.87; N, 7.23.

### 3-(3,5-di-tert-butyl-4-hydroxyphenyl)-N-(pyridine-2-yl-methyl)propanamide hydrochloride (4a)

40 mg (100%) of colorless powder of compound **4a** was obtained. Mp 230-235°C. IR, cm<sup>-1</sup>: 3638.1 (ν O-H free); 3256.7 (ν N-H); 3056.1-2871.5 (ν C-H); 1662.8 (ν C=O); 1620.4; 1539.9; 1469.0; 1434.8; 1362.5; 1233.3; 1120.4; 1035.6; 767.5. NMR <sup>1</sup>H, (400 MHz, CDCl<sub>3</sub>, δ, ppm): 1.43 (s, 18H, CH<sub>3</sub>); 2.80 (br.s, 2H, CH<sub>2</sub>); 2.88 (br.s, 2H, CH<sub>2</sub>); 4.85 (br.s, 2H, CH<sub>2</sub>); 7.00 (s, 2H, Ph); 7.76 (br.s, 1H, Py); 7.84 (s, 1H, Py); 8.29 (br.t, 1H, Py); 8.55 (br.s, 1H, Py). NMR <sup>13</sup>C (100.6 MHz, CDCl<sub>3</sub>, δ, ppm): 30.34 (C(CH<sub>3</sub>)<sub>3</sub>); 31.31 (ArCH<sub>2</sub>CH<sub>2</sub>CONH); 34.30 (C(CH<sub>3</sub>)<sub>3</sub>); 38.33 (ArCH<sub>2</sub>CH<sub>2</sub>CONH); 42.24 (CONHCH<sub>2</sub>Py); 124.90 (C2-Ar); 125.46 (C1-Ar); 129.19 (C Py); 131.04 (C Py); 135.71 (C Py); 138.95 (C3-Ar); 146.67 (C Py); 152.11 (C Py); 158.17 (C4-Ar); 173.52 (C=O). Elemental analysis, calcd for C<sub>23</sub>H<sub>32</sub>N<sub>2</sub>O<sub>2</sub>·HCl (%): C, 68.21; H, 8.21; N, 6.92. Found (%): C, 68.25; H, 8.31; N, 6.87.

### 3-(3,5-di-tert-butyl-4-hydroxyphenyl)-N-(pyridine-3-yl-methyl)propanamide hydrochloride (5a)

40 mg (100%) of colorless powder of compound **5a** was obtained. Mp 270-274°C. IR, cm<sup>-1</sup>: 3640.5 (ν O-H free); 3250.0 (ν N-H); 3073.5-2870.5 (ν C-H); 1635.8 (ν C=O); 1558.7; 1539.9; 1475.7; 1435.3; 1365.8; 1271.8; 1236.2; 1121.4; 1034.1; 786.8; 683.2. NMR <sup>1</sup>H, (400 MHz, DMSO-d<sub>6</sub>, δ, ppm): 1.33 (s, 18H, 2 Bu<sup>t</sup>); 2.43 (t, 2H, CH<sub>2</sub>, <sup>3</sup>J<sub>HH</sub>=8 Hz); 2.72 ((t, 2H, CH<sub>2</sub>, <sup>3</sup>J<sub>HH</sub>=8 Hz); 4.44 (d, 2H, CH<sub>2</sub>, <sup>3</sup>J<sub>HH</sub>=4 Hz); 6.90 (s, 2H, Ph); 7.94 (br.t, 1H, Py, <sup>3</sup>J<sub>HH</sub>=8 Hz); 8.23 (br.d, 1H, Py, <sup>3</sup>J<sub>HH</sub>=8 Hz); 8.75 (br.t, 1H, Py, <sup>3</sup>J<sub>HH</sub>=8 Hz); 8.80 (br.s, 1H, Py). NMR <sup>13</sup>C (100.6 MHz, DMSO-d<sub>6</sub>, δ, ppm): 30.47 (C(CH<sub>3</sub>)<sub>3</sub>); 31.04 (ArCH<sub>2</sub>CH<sub>2</sub>CO); 34.50 (C(CH<sub>3</sub>)<sub>3</sub>); 37.32 (ArCH<sub>2</sub>CH<sub>2</sub>CO); 45.28 (CONHCH<sub>2</sub>Py); 124.25 (C2-Ar); 125.35 (C1-Ar); 132.00 (C Py); 139.24 (C3-Ar); 139.65 (C Py); 140.40 (C Py); 140.61 (C Py); 144.01 (C Py); 151.96 (C4-Ar); 172.39 (C=O). Elemental analysis, calcd for C<sub>23</sub>H<sub>32</sub>N<sub>2</sub>O<sub>2</sub>·HCl (%): C, 68.21; H, 8.21; N, 6.92. Found (%): C, 68.70; H, 8.13; N, 6.68.



### 3-(3,5-di-tert-butyl-4-hydroxyphenyl)-N-(pyridine-4-yl-methyl)propanamide hydrochloride (6a)

40 mg (100%) of yellowish powder of compound **6a** was obtained. Mp 230–240°C. IR,  $\text{cm}^{-1}$ : 3618.8 (v O-H free); 3261.0 (v N-H); 3062.4–2871.5 (v C-H); 1669.6 (v C=O); 1598.7; 1544.2; 1505.7; 1435.3; 1370.2; 1313.3; 1230.4; 1171.1; 1029.3; 874.6; 790.7. NMR  $^1\text{H}$ , (400 MHz,  $\text{CDCl}_3$ ,  $\delta$ , ppm): 1.38 (s, 18H, 2 Bu<sup>t</sup>); 2.69 (br.s, 2H,  $\text{CH}_2$ ); 2.93 (br.s, 2H,  $\text{CH}_2$ ); 4.64 (br.s, 2H,  $\text{CH}_2$ ); 7.03 (s, 2H, Ph); 7.67 (br.s, 2H, Py); 8.57 (br.s, 2H, Py). NMR  $^{13}\text{C}$  (100.6 MHz,  $\text{CDCl}_3$ ,  $\delta$ , ppm): 30.40 ( $\text{C}(\text{CH}_3)_3$ ); 31.27 ( $\text{ArCH}_2\text{CH}_2\text{CO}$ ); 34.35 ( $\text{C}(\text{CH}_3)_3$ ); 38.26 ( $\text{ArCH}_2\text{CH}_2\text{CO}$ ); 42.58 ( $\text{CONHCH}_2\text{Py}$ ); 125.08 ( $\text{C}_2\text{-Ar}$ ); 125.38 ( $\text{C}_1\text{-Ar}$ ); 130.31 (C Py); 136.24 ( $\text{C}_3\text{-Ar}$ ); 143.95 (C Py); 150.26 (C Py); 152.16 ( $\text{C}_4\text{-Ar}$ ); 172.36 (C=O). Elemental analysis, calcd for  $\text{C}_{23}\text{H}_{32}\text{N}_2\text{O}_2\cdot\text{HCl}$  (%): C, 68.21; H, 8.21; N, 6.92. Found (%): C, 68.16; H, 8.16; N, 6.90.

### Crystallographic data collection and structure determination

All diffraction data were collected on a STOE StadiVari Pilatus 100 K diffractometer  $\lambda(\text{MoK}\alpha) = 0.71073 \text{ \AA}$ ,  $\lambda(\text{CuK}\alpha) = 1.5418 \text{ \AA}$ ,  $\omega$ -scans at 293 K.<sup>29</sup> The primary processing of the experimental data array was performed using the WinGX program package.<sup>30</sup> The structures were solved by direct methods and refined by full-matrix least-squares procedures on  $F^2$  using SHELXL97.<sup>31</sup> All non-hydrogen atoms were refined anisotropically, and hydrogen atoms were located at calculated positions and refined via the “riding model”. Crystal data and structure refinement parameters are listed in Table 1. CCDC 1960176 (**4**), 1960175 (**5**), 1960174 (**6**) contain the supplementary crystallographic data for this paper. The structures of complexes were drawn using the MERCURY CSD 3.1 program.<sup>32</sup>

**Table 1** Crystal data and the structure refinement details for compounds **4–6**

Compound	<b>4</b>	<b>5</b>	<b>6</b>
Empirical formula	$\text{C}_{23}\text{H}_{32}\text{N}_2\text{O}_2$	$\text{C}_{23}\text{H}_{32}\text{N}_2\text{O}_2$	$\text{C}_{27}\text{H}_{32}\text{N}_2\text{O}_2$
Fw	368.5	368.5	416.54
Temperature (K)	293(2)	293(2)	293(2)
Space group	$P2_1/c$	$P2_1/c$	$P2_1/c$
Syngony	Monoclinic	Monoclinic	Monoclinic
$a$ (Å)	16.3269(3)	13.4955(5)	18.2222(3)
$b$ (Å)	8.6138(3)	16.9419(5)	14.1002(2)
$c$ (Å)	16.3350(4)	9.7897(4)	17.5282(3)
$\beta$ (°)	104.667(3)	105.059(3)	97.235(2)
$V$ (Å <sup>3</sup> )	2222.44(11)	2161.44(14)	4467.78(13)
$Z$	4	4	8
$\Delta\rho_{\text{max}}/\Delta\rho_{\text{min}}$ ( $\text{e}/\text{\AA}^3$ )	0.226/-0.215	0.235/-0.169	0.263/-0.248
$\lambda$	CuK $\alpha$	CuK $\alpha$	CuK $\alpha$
$\mu$ ( $\text{mm}^{-1}$ )	0.548	0.563	0.609
$R_1/wR_2$ ( $I \geq 2_\sigma(I)$ )	0.0546/0.1336	0.0573/0.1490	0.0490/0.1273
GOOF	0.824	1.004	0.941

### Electrochemical study

All measurements were carried out under argon at room temperature. Cyclic voltammetry experiments were performed in classical three-electrode cell in  $\text{CH}_3\text{CN}$  solution with 0.05M  $\text{Bu}_4\text{NBF}_4$  as supporting electrolyte using a IPC-Win potentiostat. The number of electrons transferred was determined by comparing with the height of  $\text{Fc}^{2+}/\text{Fc}^{3+}$  wave for the same concentration and by rotating disk electrode method as well. A platinum or glassycarbon (GC) working electrode with diameter 2mm, platinum wire auxiliary electrode and aqueous  $\text{Ag}/\text{AgCl}/\text{KCl}$  (sat.) reference electrode were used. The  $\text{CH}_3\text{CN}$  prior to use was dried over  $\text{CaH}_2$  and distilled over  $\text{P}_2\text{O}_5$ .

### Antioxidant assay

#### Electrochemical DPPH test

Antioxidant activity of compounds **1–6** and **1a–6a** was studied in the reaction with stable radical 2,2-diphenyl-1-picrylhydrazyl (DPPH) in MeCN using CV method.<sup>33,34</sup> The rate of the process was monitored by the change of the DPPH reduction current intensity (with the ratio of concentrations of compounds and DPPH being 1:1 and 1:2 ( $C_0 = 10^{-3} \text{ mol}\cdot\text{L}^{-1}$ )). The CVA curves were recorded after certain periods of time (30 s, 1 and 3 min) at 100 mV/s scan rate. The values of antioxidative activity  $A = (1 - C/C_0) \cdot 100(\%)$  of compounds under study were determined for the moment of reaching steady state of reaction (“plateau”). The values of  $I_0$ , obtained by the equation of a calibrating curve at a given concentration of DPPH were used for the plotting the kinetic curves and determining the stoichiometry values.

#### Spectrophotometrical DPPH assay

The radical scavenging activity was evaluated using the radical 2,2-diphenyl-1-picrylhydrazyl (Sigma-Aldrich) by spectrophotometry at  $\lambda_{\text{max}} = 517 \text{ nm}$  according the known procedure.<sup>35</sup> The reaction was performed in 1cm glass cuvettes. The reaction mixture contained DPPH (0.75 ml, 0.2mM) and a solution of the test compound in EtOH (0.75 ml, 0.2mM). The reaction was monitored for 20 h. The data were calculated using the Microsoft Excel 2010. The antioxidant activity was calculated as percentage of reduced DPPH according to the formula  $I (\%) = (A_0 - A_1)/A_0 \cdot 100$ , where  $A_0$  is the absorbance of the control 0.1mM DPPH in EtOH,  $\epsilon_{\text{DPPH}} = 1.15 \cdot 10^4$ ,  $A_1$  is the absorbance of the reaction mixture in the presence of the test compound.

#### CUPRAC assay

The ability of the compounds to one-electron transition was measured by means of reduction of complex of 2,9-dimethyl-1,10-phenanthroline (neocuproine, Sigma-Aldrich, 98%) with copper by spectrophotometry at  $\lambda_{\text{max}} = 450 \text{ nm}$ . The known procedure<sup>36</sup> was modified for plate spectrophotometer. The reaction was performed in plate wells (96 wells). The volume of reaction mixture inside one well was 0.2 ml and consisted of 0.05 ml of ammonium acetate buffer (pH 7.0), 0.05 ml of 10mM  $\text{CuCl}_2$  solution in methanol, 0.05 ml of 7.5mM neocuproine solution in methanol and 0.05 of 0.5mM tested compound solution in methanol. The results were compared to Trolox and expressed in trolox equivalent antioxidant capacity (TEAC) and calculated according to the formula  $\text{TEAC} = A_1/A_0$ , where  $A_1$  is the absorbance of the reaction mixture in the presence of the tested compound and  $A_0$  is the absorbance of the solution of trolox of the same concentration.

## NBT assay

The effects of compounds **1-6** and **1a-6a** on enzymatic generation of the superoxide radical anion  $O_2^{\cdot-}$  in the xanthine-xanthine oxidase system were estimated by the amount of reduced tetrazolium blue into formazan.<sup>37</sup>

The composition of the reaction mixture in 96 well plate was as follows: carbonate buffer (270  $\mu$ l, 40mM, pH 10.0) containing EDTA (0.1mM), a solution of xanthine (6  $\mu$ l, 10mM) in carbonate buffer, a 0.5% bovine serum albumin (3  $\mu$ l) in water, nitro blue tetrazolium chloride (NBT, 3  $\mu$ l, 2.5mM) in water, and a solution of the compound under study in DMSO (6  $\mu$ l of 5mM concentration). Xanthine oxidase (12  $\mu$ l, 0.004 units) in buffer was added to the mixture at rt and the absorption at 560 nm ( $\lambda_{\max}$  blue formazan) was recorded by Thermo Scientific Multiskan Go microplate spectrophotometer for 600 s. The control experiment was performed in the presence of DMSO (6  $\mu$ l) without compound. All experiments were performed in triplicate.

Inhibition I (%) =  $(1 - A_i/A_0) \times 100\%$ , where  $A_i$  is the absorbance in the presence of the testing compound at the end of the reaction (600 s),  $A_0$  is the absorbance of the blank solution.

## Inhibition of lipoygenase (LOX I-B)

The lipoygenase activity was evaluated spectrophotometrically.<sup>38</sup> The concentrations of linoleic acid oxidation products, isomeric hydroperoxides, were measured at  $\lambda_{\max} = 234$  nm ( $\epsilon = 25000 \text{ L mol}^{-1} \text{ cm}^{-1}$ ) with a 96-well microplate spectrophotometer Multiskan Go (Termo Scientific, USA). The analyzed solution contained 30  $\mu$ l borate buffer (pH 9.0), 100  $\mu$ l linoleic acid (0.45mM) in borate buffer, 3  $\mu$ l 1mM solution of test compound in DMSO. The reaction was initiated by the addition of 17  $\mu$ l of lipoygenase (500 U) solution in borate buffer.

The measurements were performed for 5 min at 20°C.

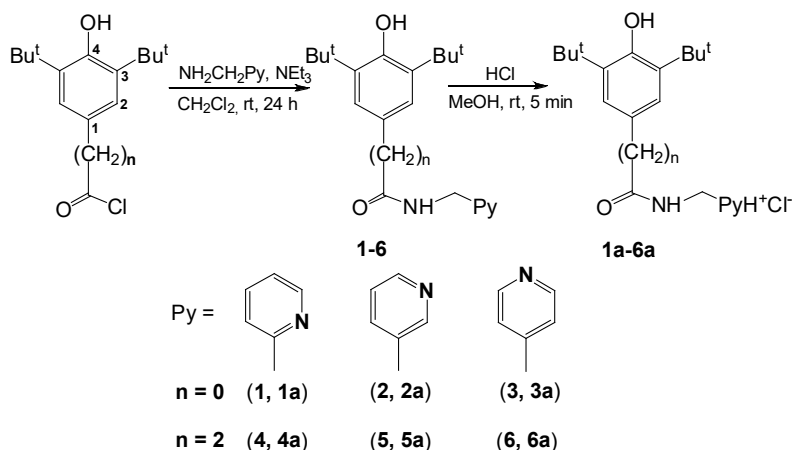
The inhibition rate I (%) of lipoygenase was determined by the formula:

$$I (\%) = (v_0/v_0') \cdot 100\%,$$

where  $v_0$  and  $v_0'$  are initial rates of the enzymatic reaction in the presence and absence (control) of the compounds under study, respectively.

The initial rate ( $v_0$  and  $v_0'$ ) was calculated by the formula

$$v_0 = \Delta C/\Delta t = \Delta A/(\Delta t \cdot \epsilon) = \text{tg}\alpha/(\Delta t \cdot \epsilon),$$



**Scheme 1** Synthesis of amides **1-6** and hydrochlorides **1a-6a**.

where  $A_0$  is the absorbance of the control solution, and  $A_i$  is the absorbance of the reaction mixture in the presence of the tested compound 5 min after the beginning of the reaction. All experiments were performed in triplicate.

## Mitochondrial lipid peroxidation

Lipid peroxidation in mitochondrial suspension was followed by the accumulation of substances that reacted with thiobarbituric acid (TBARs), and monitored spectrophotometrically according to the procedure described previously.<sup>39</sup> Mitochondrial membranes lipid peroxidation was induced by using  $\text{FeNH}_4(\text{SO}_4)_2 \cdot 12\text{H}_2\text{O}$  ( $\text{Fe}^{3+}$ ; 0.5mM) or *tert*-butylhydroperoxide (BHP) as an oxidizing agent.

## Mitochondria preparation and assays

Mitochondria were isolated by conventional differential centrifugation from the livers of adult Wistar strain rats fasted overnight in 5mM HEPES buffer (pH 7.4) containing 210mM mannitol, 70mM sucrose, and 1mM EDTA.<sup>40</sup> Since mannitol binds hydroxide ions, it was omitted during the final centrifugation and resuspension of mitochondria in experiments with lipid peroxidation estimation. The mitochondrial fraction contained 130-150 mg of protein per liver. Mitochondria were stored at 4°C. Functional activity of rat liver mitochondria remained constant during 3-4 h. Protein concentrations were determined by the biuret assay using bovine serum albumin as a standard.<sup>41</sup> Mitochondrial potential and mitochondrial swelling were performed in accordance with our previous work.<sup>42</sup>

## MTT assay

The toxicity of compounds was studied on primary cultures of rat brain cortex neurons with standard MTT assay.<sup>43,44</sup>

## Results and discussion

### Chemistry and structural study

Amides **1-6** with various length of a linker and different position of a nitrogen atom in the pyridine ring were synthesized by the interaction of acids chlorides with different picolylamines in the presence of  $\text{NEt}_3$  for accepting of liberated HCl (Scheme 1). Reactions were carried out in  $\text{CH}_2\text{Cl}_2$  under room temperature to give stable products with 45-90% yields as colorless powders. For the hydrophilization of compounds amides **1-6** were treated with 3 molar equivalents of conc. HCl in MeOH by previously described method<sup>45</sup> to yield corresponding hydrochlorides **1a-6a** after removing of solvent. Compounds obtained were stable in air and in solutions and were characterized by IR,  $^1\text{H}$  and  $^{13}\text{C}$  NMR spectroscopy and elemental analysis.

The recrystallization of compounds **4–6** from the mixture of  $\text{CH}_2\text{Cl}_2$  - petroleum ether gave the monocrystals. The crystal and molecular structures of compounds **4–6** were determined by X-ray diffraction. The crystallographic characteristics and selected bond lengths and bond angles for compounds **4–6** are summarized in Tables 1, 2. Compounds **4** and **5** in the solid state were found to be monomers (Figure 1A, 1B). In the case of **4** the angle between the planes of benzene and pyridine rings is  $84.08^\circ$ . The intermolecular hydrogen bonds  $\text{N2-H2} \cdots \text{N1}$  and  $\text{O1-H1} \cdots \text{O2}$  with the distances  $\text{H2} \cdots \text{N1} = 2.132 \text{ \AA}$  and  $\text{H1} \cdots \text{O2} = 1.795 \text{ \AA}$  respectively were detected.

In the structure of **5** the angle between the planes of benzene and pyridine rings was  $19.61^\circ$ . The intermolecular hydrogen bonds  $\text{N1-H1}$

$\cdots \text{O1}$  and  $\text{O2-H11} \cdots \text{N2}$  with the distances  $\text{H1} \cdots \text{O1} = 1.813 \text{ \AA}$  and  $\text{H11} \cdots \text{N2} = 2.234 \text{ \AA}$  respectively were found.

Compound **6** appeared to be a homodimer (Figure 1C). Two monomers are arranged in such a way that pyridine ring of one molecule is located opposite to the hindered phenol fragment of another one resulting in the formation of hydrogen bonds  $\text{O1-H12} \cdots \text{N2A}$  and  $\text{O1A-H11A} \cdots \text{N2}$  with the distances  $\text{H12} \cdots \text{N2A} = 2.082 \text{ \AA}$  and  $\text{H11A} \cdots \text{N2} = 1.998 \text{ \AA}$  respectively. Also, the intermolecular hydrogen bonds  $\text{N1-H11} \cdots \text{O2A}$  and  $\text{N1A-H12A} \cdots \text{O2}$  with the distances  $\text{H11} \cdots \text{O2A} = 1.911 \text{ \AA}$  and  $\text{H12A} \cdots \text{O2} = 1.865 \text{ \AA}$  respectively were revealed.

**Table 2** Selected bond lengths (Å) and angles (°) for compounds **4–6**

Bond lengths (Å)					
4		5		6	
O1–C1	1.382(2)	O1–C1	1.227(2)	O1–C1	1.3725(19)
O1–H1	0.96(4)	O2–C7	1.376(3)	O1–H12	0.84(3)
O2–C11	1.228(2)	O2–H11	0.92(3)	O2–C17	1.234(2)
N1–C13	1.335(3)	N1–C1	1.328(3)	N1–C17	1.327(2)
N1–C17	1.340(3)	N1–C18	1.456(3)	N1–C18	1.449(2)
N2–C11	1.336(3)	N1–H1	0.99(2)	N1–H11	0.92(2)
N2–C12	1.456(3)	N2–C22	1.321(5)	N2–C22	1.324(2)
N2–H2	0.86(3)	N2–C23	1.323(4)	N2–C21	1.325(2)
Angles (°)					
C1–O1–H1	109(2)	C7–O2–H11	116(2)	C1–O1–H12	118.1(18)
C13–N1–C17	117.3(2)	C1–N1–C18	122.30(19)	C17–N1–C18	121.87(15)
C11–N2–C12	121.8(2)	C1–N1–H1	119.0(13)	C17–N1–H11	120.5(13)
C11–N2–H2	120.3(16)	C18–N1–H1	118.7(13)	C18–N1–H11	117.1(13)
C12–N2–H2	117.8(16)	C22–N2–C23	116.6(3)	C22–N2–C21	115.85(15)
O2–C11–N2	120.9(2)	O1–C1–N1	122.5(2)	O2–C17–N1	121.97(16)

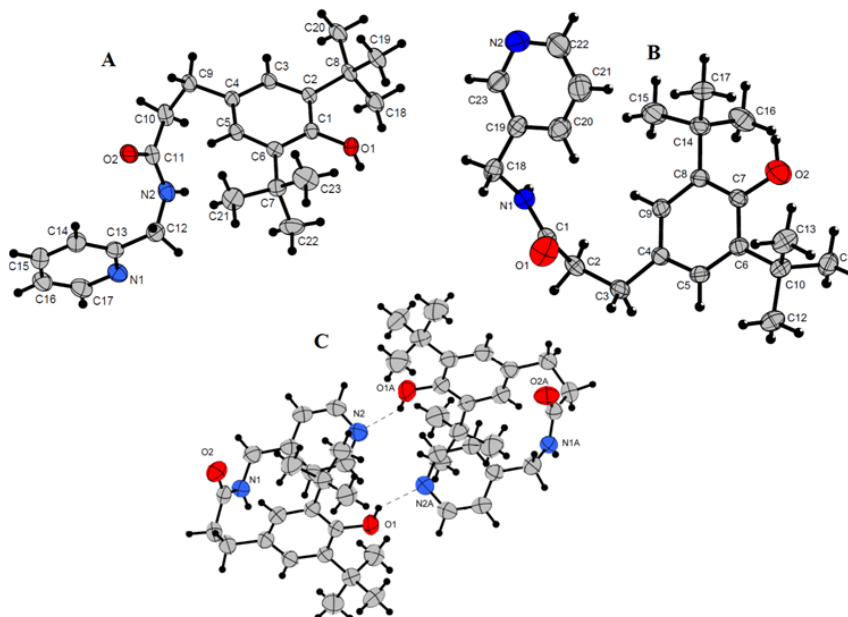


**Figure 1** Molecular structures of compounds **4** (A), **5** (B), **6** (C). Thermal displacement ellipsoids are given at the 50% probability level. Hydrogen atoms are omitted for clarity.

## Formation of phenoxyl radicals

Phenoxyl radicals generated by the oxidation of corresponding *para*-substituted di-*tert*-butyl phenols were described previously.<sup>46</sup> Stability of radicals was influenced by electron-donor and electron-withdrawing properties of *para*-substituents of phenol group.

The formation of radicals during chemical oxidation of compounds **1-6** (PbO<sub>2</sub> in toluene) was proved by EPR spectroscopy. The X-band

EPR spectra measured at 293 K show the spin density distribution in the organic ligand. The spectra of radicals **1-3** are triplets corresponding to the coupling of the unpaired electron with two equivalent meta-protons (<sup>1</sup>H, S = 1/2) of the phenoxyl ring while radicals derived from **4-6** demonstrate also hyperfine coupling constants of two equivalent protons of benzyl CH<sub>2</sub> group (Figure 2). The parameters of the EPR spectra of radicals (Table 3) are close to those of similar phenoxyl radicals.<sup>22</sup>

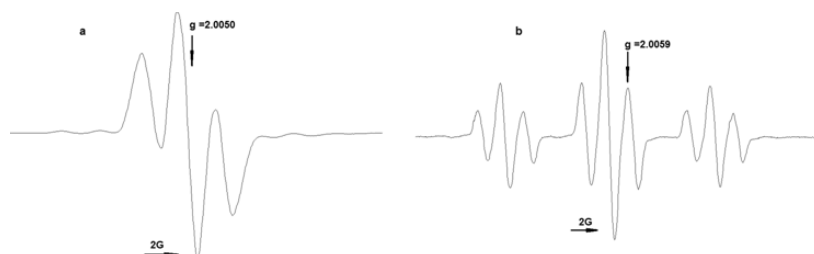


**Figure 2** EPR spectra of radicals generated from compounds **2** (a) and **4** (b) by PbO<sub>2</sub> in toluene (293 K).

**Table 3** The isotropic g-value and hyperfine coupling constants (a) for radicals **1-6**

Compound	g-value	a <sub>2H</sub> (Ar), mT	a <sub>2H</sub> (ArCH <sub>2</sub> ), mT
1	20,054	0.18	-
2	2.005	0.215	-
3	2.0058	0.215	-
4	2.0056	0.17	0.79
5	2.0053	0.17	0.78
6	2.0059	0.17	0.78

The radicals were stable in solutions at room temperature under anaerobic conditions. The intensity of radicals generated from **1-3** and bearing electron-withdrawing amide fragment in *para*-position which can participate in delocalization of unpaired electron is one order higher than that of radicals from **4-6** possessing electron-donor alkyl moiety. The similar effects have been observed for phenoxyl radicals containing transition metals.<sup>47</sup>

## Electrochemical study

Voltammetric methods have often been applied for elucidation of activity mechanism of natural and synthetic phenolic antioxidants.<sup>48,49</sup> In this work the redox properties of compounds **1-6** as well as hydrochlorides **1a-6a** were measured and their electrochemical behavior was studied by cyclic voltammetry (CV) method using Pt working electrode. The redox potentials values are summarized in Table 4.

The redox behavior of phenols under study strongly depends on the structure of substituent in *para*-position and the length of hydrocarbonyl linker. Compounds **1-3** shows wide one-electron oxidation peak on voltammogram at potentials E<sub>a</sub> = 1.2-1.27 V (Figure 3). The irreversibility of this wave points out the EC mechanism (electron transfer followed by the fast-chemical reaction). These data are in accordance with results obtained in<sup>50</sup> concerning electrochemical behavior of acetanilide, propanil and *N,N*-diphenylacetamide indicating the involvement of amide nitrogen atom in oxidation.

**Table 4** The redox potentials values (E<sub>a</sub>, V) of compounds **1-6** and **1a-6a** (CH<sub>3</sub>CN, 5 · 10<sup>-2</sup> M n-Bu<sub>4</sub>NBF<sub>4</sub>, Pt electrode, scan rate 100 mV/s, via Ag|AgCl|KCl(sat.))

Compound	Oxidation potential, V	
	E <sub>a1</sub>	E <sub>a2</sub>
<b>1</b>	1.2	-
<b>2</b>	1.27	-
<b>3</b>	1.24	-
<b>4</b>	1.23	1.57
<b>5</b>	1.05	1.42
<b>6</b>	-	1.7
<b>1a</b>	1.2	1.65
<b>2a</b>	1.13	-
<b>3a</b>	1.2	1.7
<b>4a</b>	1.14	-
<b>5a</b>	1.1	-
<b>6a</b>	0.98	1.6
<b>BHT*</b>	1.63	-

\*Butylated hydroxytoluene

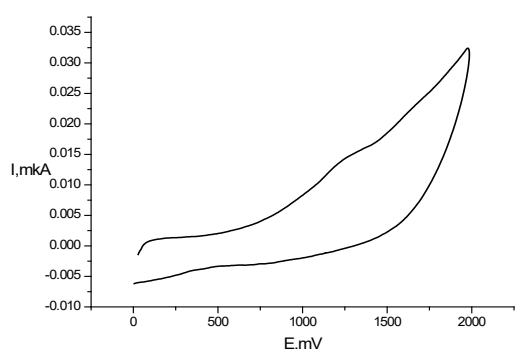


**Figure 3** CV of compound **2** in anodic range ( $C=1\text{ mM}$ , Pt electrode,  $50\text{ mM TBABF}_4$ ,  $\text{CH}_3\text{CN}$ , scan rate  $100\text{ mV/s}$ , vs.  $\text{Ag/AgCl}$ )).

At the same time, the introduction of  $-(\text{CH}_2)_2$ - linker in compounds **4** (Figure 4) and **5** leads to the marked change of electrochemical behavior: the two one-electron irreversible peaks of oxidation at the anodic region are displayed in the potential range  $1.05\text{--}1.57\text{ V}$ .

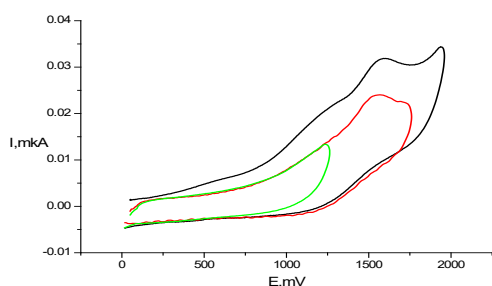
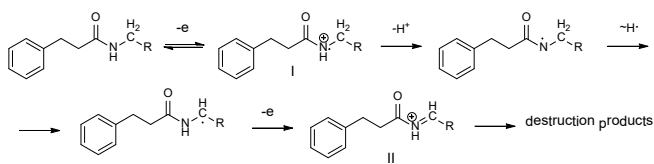


**Figure 4** CV of compound **4** ( $C=1\text{ mM}$ , Pt electrode,  $50\text{ mM TBABF}_4$ ,  $\text{CH}_3\text{CN}$ , scan rate  $100\text{ mV/s}$ , vs.  $\text{Ag/AgCl}$ )).

The first peak on CV curves of compounds **4** and **5** (at less anodic potentials  $E_a = 0.96\text{--}1.30\text{ V}$ ) can be associated with N-centered one-electron oxidation of amide group, resulting in formation of radical cation **I** (Scheme 2) and followed by fast deprotonation, as it was observed in case of ferulic and caffeic acid amides.<sup>51,52</sup> The second peak at  $1.42\text{--}1.57\text{ V}$  corresponds to further one-electron oxidation of methylene fragment that leads to the formation of N-acylium cation **II**.<sup>53</sup>



**Scheme 2** Feasible mechanism of electrochemical oxidation of compounds **4-6**.

Cyclic voltammograms of compounds were also recorded at different sweep rates. Linear plots of peak current ( $I_p$ ) as a function of the square root of scan rate ( $n$ ) were obtained indicating that oxidation processes are diffusion controlled.<sup>54</sup>

However, compound **6** demonstrate different pattern of electrochemical activity by showing irreversible two-electron oxidation peak at  $E_a = 1.7\text{ V}$  (Figure 5).

In the case of compounds **1a-6a** the one-electron peak at  $1.0\text{--}1.2\text{ V}$  appears as well what obviously corresponds to  $\text{Cl}^-/\text{Cl}^0$  oxidation.<sup>55</sup> The peak corresponding to oxidation of phenol moiety is observed only for compounds **1a**, **3a** and **6a** (Figure 5) at more positive potentials than

in case of corresponding phenols **1**, **3**, **6** (Table 4). This phenomenon may be due to the considerable shift of oxidation potential to anodic range because of electron-withdrawing influence of positively charged pyridinium fragment.

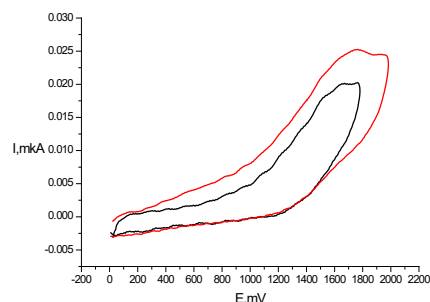


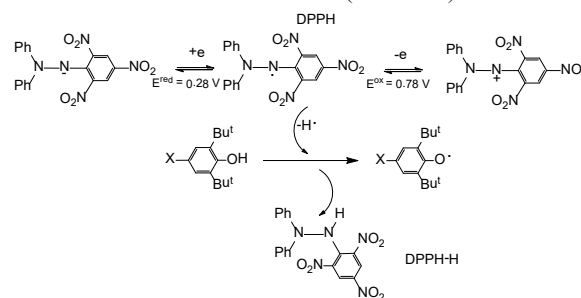
**Figure 5** CV of compound **6** ( $C=1\text{ mM}$ , Pt electrode,  $50\text{ mM TBABF}_4$ ,  $\text{CH}_3\text{CN}$ , scan rate  $100\text{ mV/s}$ , vs.  $\text{Ag/AgCl}$ )).

## Evaluation of antioxidant activity

The antioxidant properties of compounds **1-6** were studied in model reactions. Redox properties and radical scavenging ability were evaluated by cyclic voltammetry in 2,2-diphenyl-1-picrylhydrazyl (DPPH) test. Affinity to one-electron transfer was measured by CUPRAC-test. The ability to interact with superoxide radical anion was measured using the xanthine-xanthine oxidase system. The inhibition of oxidation of linoleic acid by lipoxygenase *in vitro* and rat liver lipid peroxidation *ex vivo* was estimated.

## Electrochemical DPPH-test

Oxidation peaks for studied compounds are observed at more anodic region (Table 4) than that of 2,2-diphenyl-1-picrylhydrazyl radical (DPPH) for which the first reduction wave appeared at peak potential  $0.28\text{ V}$ .<sup>56</sup> The cyclic voltammogram of DPPH (Figure 6) in  $\text{CH}_3\text{CN}$  displays two one-electron reversible peaks that correspond to oxidation and reduction of this radical (Scheme 3).<sup>57</sup>



**Scheme 3** Mechanism of radical scavenging activity of 2,6-di-*tert*-butylphenols with DPPH.

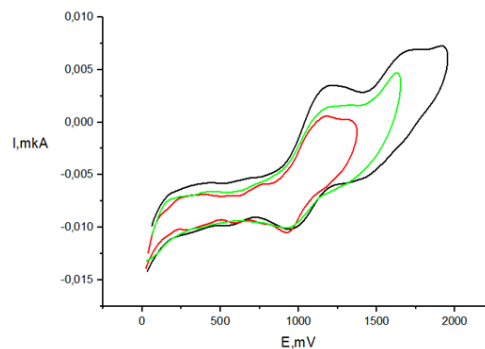


**Figure 6** CV of compound **1a** ( $C=1\text{ mM}$ , GC electrode,  $50\text{ mM TBABF}_4$ ,  $\text{CH}_3\text{CN}$ , scan rate  $100\text{ mV/s}$ , vs.  $\text{Ag/AgCl}$ )).



Therefore, CV method can be used in order to study antioxidant activity in reaction of H-transfer to DPPH. The fact that the redox potentials values of **1-6** and **1a-6a** do not overlap with potentials of DPPH oxidation/reduction allows one to apply the CV method for estimation of antioxidant activity.<sup>33,34</sup>

In the presence of the antioxidants the current values of both peaks decreased (Figure 7).

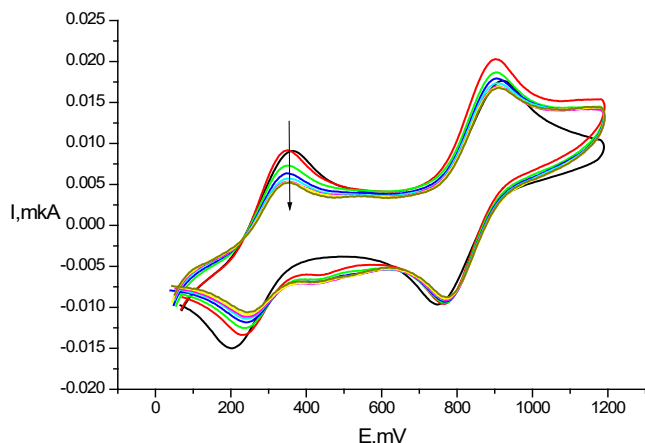


**Figure 7** Voltammogram of 1 mM DPPH in the presence of 0.5 mM compound **6** on Pt electrode in  $\text{CH}_3\text{CN}$  ( $v=100\text{mV/s}$ , 5 mM  $\text{Bu}_4\text{NBF}_4$ , time of reaction 30 min,  $\text{Ag}|\text{AgCl}||\text{KCl}$  (sat.)).

According to the Randles-Shevchik equation at specific electrode surface area and potential scan rate the ratio of radical reduction and oxidation peak currents during the reaction is equal to the concentration ratio  $I/I_0 = C/C_0$  ( $I_0$  is the value current without antioxidant,  $I$  is the current at a chosen time of reaction). Hence, we used this relation to quantitatively estimate the antioxidant efficiency (AOE) as the percentage of reacted DPPH:

$$\text{AOE} = (1 - I_{\text{fin}}/I_0) \times 100 (\%) = (1 - C_{\text{fin}}/C_0) \times 100 (\%),$$

where  $C_0$  is the starting DPPH concentration,  $C_{\text{fin}}$  is DPPH concentration in the end of the reaction.

This simple method has some advantages compared to spectrophotometrical test. Electrochemical test allows to use higher concentrations of antioxidants that leads to the increase of reaction rate with DPPH. The compounds **1-3** did not show any significant scavenging activity. Even at concentrations ratio DPPH/compound 1:1 ( $C = 1\text{mM}$ ) the amount of reacted radical was about 6-9%. But in the case of **4-6** the activity changes dramatically. Thus at 1:1 ratio the amount of reduced DPPH was close to 100%. The compounds **4** and **5** demonstrated high activity: at DPPH/compound concentrations ratio 2:1 the amounts of DPPH quenched were 34% and 22% (at reaction time 30 min). After 48 h these amounts reached values of 67% and 58%, respectively, that points out the stoichiometry of reaction more than 1. According to these data compounds **4-6** are antioxidants with prolonged action effect. Therefore, the length of the linker between phenol and amide fragments strongly affects the radical scavenging activity of presented compounds.

The activity of compounds **1a-6a** in electrochemical tests differs slightly from the activity of compounds **1-6**. At concentrations ratio 1:1 the compounds **1a-3a** very slowly react with DPPH (the amount of radical quenched is 3-5% even after 24 h of reaction proceeding). But the compounds **4a-6a** demonstrated high activity: at equimolar

concentrations DPPH reacted completely ( $\text{AOE} = 100\%$  at reaction time 24 h). Thereby, the results of electrochemical test can be compared with data obtained spectrophotometrically as well.

### Spectro photometrical DPPH-test

DPPH is violet-colored stable radical with the maximum of absorbance at 517 nm while the 2,2-diphenyl-1-picrylhydrazine (DPPH-H) is pale yellow. This radical is a useful reagent for the investigation of the radical scavenging activity of phenols, catecholes, etc. The amount of reacted DPPH can be defined by method suggested by W. Brand-Williams.<sup>58</sup> The accepted reaction mechanism at the first stage includes hydrogen atom abstraction from an antioxidant to give DPPH-H and corresponding radical followed by secondary transformations. The reaction of 0.1 mM of synthesized compounds in ethanol with equimolar concentration of DPPH involves a color change from violet to yellow, which can be monitored spectrophotometrically by measuring the decrease in absorbance for 20 h at 517 nm (Figure 8).

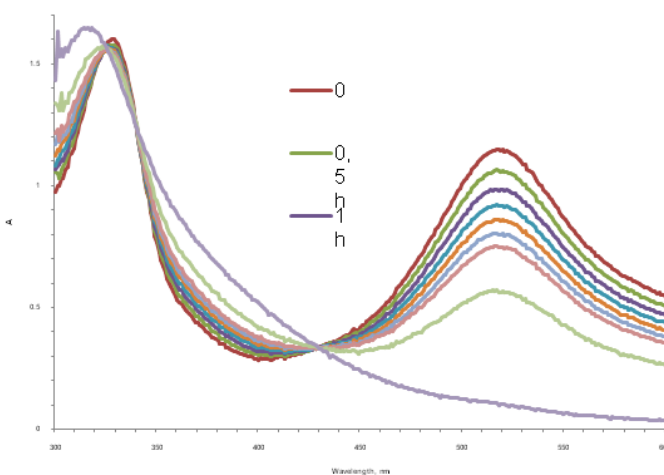


**Figure 8** Changes in UV-vis spectrum of DPPH (0.1 mM) in the presence of 0.1 mM compound **6** in  $\text{EtOH}$ ,  $20^\circ\text{C}$ .

The percentage of reduced DPPH in the presence of test compounds was increased with time compared to control (0.1 mM DPPH) at the same time spans (Table 5). The amount of reduced DPPH was lower for compounds **1-3** and **1a-3a** than that of their analogues **4-6** and **4a-6a** due to the difference in chemical structure of phenoxy radicals which in the case of  $-(\text{CH}_2\text{CH}_2)$ -bearing radical can participate in further reactions with DPPH as it was demonstrated previously.<sup>43</sup> It can be noticed that after 20 h of reaction the percentage of reduced DPPH by compounds was much higher for compounds **4-6**, **4a-6a** in comparison with control (Figure 9). The antioxidant abilities of tested compounds were compared to that of BHT.

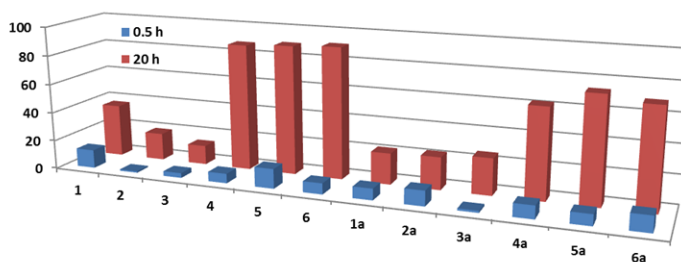


**Figure 9** Comparison of the amount of reduced DPPH (%) in the presence of compounds **1-6** and **1a-6a** on 0.5 h and 20 h.

**Table 5** The amount of reduced DPPH (%) for compounds **1-6** and **1a-6a**

Compound	Time, h							
	0.5	1	1.5	2	2.5	3	5	20
<b>1</b>	12.7	14.3	15.5	16	17.2	17.8	18.5	36.6
<b>2</b>	1	3.6	5.3	6.6	8.3	9.2	12	18.9
<b>3</b>	3.3	4.9	6.1	7	8.1	9	11.8	13.3
<b>4</b>	6.6	18.8	27.8	35.3	41.9	47.1	70.8	87.7
<b>5</b>	13.6	29	40.3	48.7	55.7	61	77.1	89.4
<b>6</b>	7.6	14.4	20.1	25.3	30.3	34.9	50.4	90.9
<b>1a</b>	7.9	9.7	11	12.4	13.7	15	17	21.6
<b>2a</b>	10.5	11.9	13	14.9	15	16.6	16.6	22.5
<b>3a</b>	1.4	3.5	5.4	6.3	7.9	9	13.1	25.4
<b>4a</b>	9	13.2	17	20.5	23.7	26.9	34.7	62.4
<b>5a</b>	7.7	11.8	15.7	19.5	23	26.4	37	73.3
<b>6a</b>	11.1	15.1	18.9	22.2	25.4	28.4	38.1	69.2
<b>BHT</b>	1.3	3.4	5.3	6.3	7.8	8.9	13.2	22.6

In the case of  $-(CH_2CH_2)_n$  linker such ability is restricted and the antioxidant activity of amides from phenol containing propionic acid was higher. To conclude the presence of the linker between phenol and amide fragments influences the anti-radical activity of compounds.

Thus, the data of electrochemical and spectrophotometrical DPPH tests correlate well enough (considering the difference of the reacting substances concentrations).

#### One-electron transfer capability (CUPRAC test)

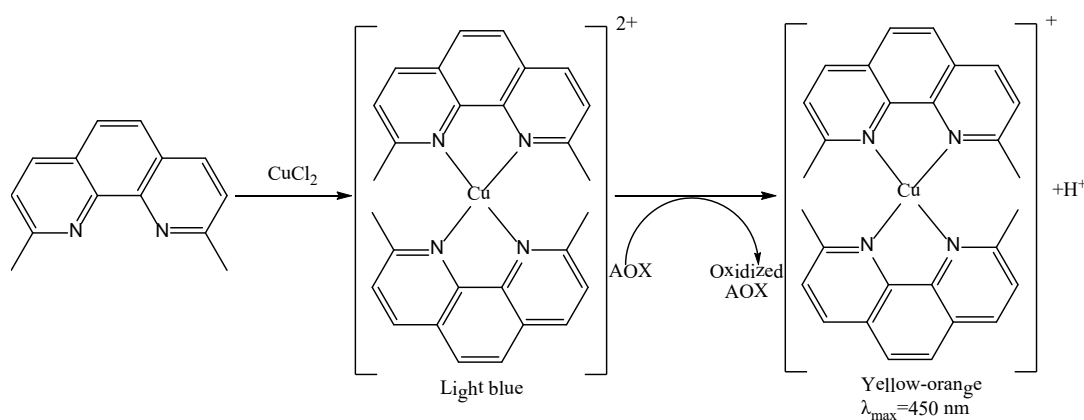
Capability of the compounds to abstract one-electron makes them the potential antioxidants. The one-electron transfer capacity of compounds was examined as  $Cu^{2+}$  complex with 2,9-dimethyl-1,10-phenanthroline (neocuproine) reducing ability in method proposed by Apak et al. (Scheme 4).<sup>36</sup> Antioxidant activity of compounds is compared to standard antioxidant trolox (6-hydroxy-2,5,7,8-tetramethylchroman-2-carboxylic acid) as an analogue of  $\alpha$ -tocopherol. While  $Cu^{2+}$  complex is light blue the reduction with

antioxidant changes its color to yellow orange with  $\lambda_{max}$  at 450 nm that can be detected spectrophotometrically.

Results were presented in Trolox equivalents (TEAC–Trolox equivalent antioxidant capacity). The comparison of TEAC values allows one to conclude that the pyridine fragment plays a significant role in electron transfer to the  $Cu^{2+}$  ion (Table 6). The capability to one-electron transfer was higher for *ortho*-substituted pyridines.

#### Superoxide radical anion scavenging activity (NBT assay)

The ability of tested compounds to reduce superoxide radical anion  $O_2^{\cdot -}$  generated in enzymatic oxidation of xanthine by xanthine oxidase to uric acid was studied.<sup>37</sup> The percentage of reduced radical anion was defined spectrophotometrically by detection of blue formazan formation ( $\lambda_{max}$  560 nm) from nitro blue tetrazolium (NBT). It was found that all the compounds are frugal reducers of  $O_2^{\cdot -}$  with activity percentage within 2-19% range (Table 6).

**Scheme 4** Formation of copper complex and its reduction in the presence of antioxidant (AOX).

**Table 6** TEAC in CUPRAC test; A (%) -reduced superoxide radical anion in percentage of control; I (%) -inhibition of linoleic acid oxidation by LOX 1-B for compounds **1-6** and **1a-6a**

Compound	TEAC*	NBT assay ** I (%)	Inhibition of LOX 1B*** I (%)
<b>1/1a</b>	0.89 / 1.21	10.7 / 12.4	7.6/19.2
<b>2/2a</b>	0.29 / 0.54	8.8 / 5.0	8.5/1.7
<b>3/3a</b>	0.35 / 0.61	19.1 / 5.6	12.0/1.0
<b>4/4a</b>	1.71 / 1.35	2.9 / 2.1	1.4/5.7
<b>5/5a</b>	1.00 / 1.05	4.1 / 13.0	5.3/7.3
<b>6/6a</b>	1.10 / 1.56	7.0 / 11.9	2.6/0.6
<b>BHT</b>	1.1	10.3	50****

\*-concentration of compound 0.5mM; \*\* - 5mM; \*\*\* - 1mM; \*\*\*\*-0.8mM

### Lipoxygenase inhibitory assessment

Lipoxygenases catalyze regio- and stereoselective oxidation of polyunsaturated fatty acids containing one or more (1Z,4Z) pentadiene fragments to the corresponding hydroperoxides.<sup>59</sup> This reaction is the first step in the biosynthesis of leukotrienes - mediators of various inflammatory processes and allergic reactions participating in the pathogenesis of neoplastic diseases, asthma, and atherosclerosis.<sup>60</sup> Moreover, the side products of this reaction are superoxide radical anion and hydrogen peroxide. Thereby, lipoxygenase is an important pharmaceutical target and many attempts have been made to find a selective lipoxygenase inhibitor.<sup>61,62</sup> Soybean lipoxygenase 1-B (LOX 1-B) is frequently used as a model enzyme in the study of homological lipoxygenase family. In particular, 5-lipoxygenases acting in the human body and LOX-1-B catalyze oxidation of linoleic acid to isomeric hydroperoxyoctadienoic acids. Since tested compounds possess antioxidant properties they have been examined as LOX 1-B inhibitors.

The reaction of linoleic acid oxidation was monitored spectrophotometrically at  $\lambda_{\max}$  234 nm corresponding to maximum absorption of octadienoic acids hydroperoxides. The activity of the compound as a lipoxygenase inhibitor was characterized by the degree of inhibition I (%) of hydroperoxides accumulation after 5 min incubation with the 1mM of test compounds (Table 6). It was found that all compounds are mild inhibitors of LOX-1B with I ranged between 1-19%.

### Influence of compounds on lipid peroxidation of rat liver homogenates and mitochondrial functions

In this study the influence of tested compounds on lipid peroxidation (LP) in rat liver homogenates induced by  $\text{Fe}^{3+}$  and *tert*-butylhydroperoxide ('BHP) was followed. The accumulation of products that reacted with thiobarbituric acid (TBARS) was monitored spectrophotometrically at  $\lambda_{\max}$  530 nm.<sup>63</sup> The  $\text{IC}_{50}$  values (the concentration of a compound required for achieving *in vitro* 50% inhibition of the reaction) are given in Table 7.

Among tested compounds in 'BHP induced LP the most effective antioxidants with  $\text{IC}_{50}$  values ranging between 0.5–0.9  $\mu\text{M}$  were compounds with  $-(\text{CH}_2\text{CH}_2)-$  spacer **4-6**. However, their effect on  $\text{Fe}^{3+}$  induced lipid peroxidation is less pronounced. Antioxidant activity of **4-6** was 6 times higher than that of **1-3**.

Mitochondria play the key role in  $\text{O}_2$ -dependent energetic support of cells and accordingly in the production of ROS, participate in the

apoptotic cascade by serving as a convergent center of apoptotic signals originated from both the extrinsic and intrinsic pathways. The change in mitochondrial potential is an indicator of both the activity of the respiratory chain of mitochondria and the induction of proapoptotic mitochondrial permeability transition pore opening.<sup>64</sup> We examined the influence of compounds on mitochondrial potential in the presence of complex I and complex II substrates (Table 7) and on Ca-induced mitochondrial swelling as the direct indicator of mitochondrial permeability transition pores opening.

**Table 7** Influence of compounds on 'BHP and  $\text{Fe}^{3+}$  induced lipid peroxidation

Compound	$\text{IC}_{50}$ , $\mu\text{M}$	
	$\text{Fe}^{3+}$	'BHP
<b>1</b>	22.8±6.4	11.1±3.9
<b>2</b>	14.0±2.8	5.3±1.0
<b>3</b>	24.1±6.4	3.7±1.1
<b>4</b>	3.4±0.8	0.9±0.2
<b>5</b>	3.4±0.7	0.5±0.1
<b>6</b>	3.9±1.0	0.8±0.2
<b>1a</b>	11.4±2.0	10.9±1.8
<b>2a</b>	6.0±2.6	26.7±7.1
<b>3a</b>	6.2±2.2	19.8±6.2
<b>4a</b>	0.9±0.6	2.4±0.5
<b>5a</b>	4.0±3.2	1.2±0.2
<b>6a</b>	4.9±1.3	1.7±0.4
<b>BHT</b>	0.76±0.11	3.98±0.75

It was shown that all compounds in concentration up to 30  $\mu\text{M}$  don't affect the membrane potential  $\Delta\phi$  and Ca-induced swelling of isolated rat liver mitochondria that is an important feature of pharmaceutical agents. Further studies of the effect of the compounds (at 10  $\mu\text{M}$ ) on the viability of rat brain cortical neurons in primary culture also did not reveal the significant cytotoxicity of these compounds (data not shown) and these results allow us to propose the future investigations of modified 2,6-di-*tert*-butylphenols with pyridine moiety as non-toxic antioxidant as cytoprotectors against oxidative stress.

## Conclusion

The synthesis, structures, redox properties and *in vitro* antioxidant effects of new pyridine with 2,6-di-tert-butylphenols groups and their water-soluble hydrochlorides are presented. The obtained compounds are characterized by NMR, IR, X-ray and elemental analysis. Antioxidant activity is evaluated using model reactions of hydrogen atom abstraction (DPPH-test) and one-electron reduction (CUPRAC-test), cyclic voltammetry (CV) as well as by biochemical assays. It was shown that compounds possess radical scavenging activity of prolonged action due to the formation of relatively stable phenoxyl radicals as evidenced by EPR. The compounds are found to be mild inhibitors of *lipoxigenase*. Both lipophilic and hydrophilic forms demonstrate high antioxidant activity in induced lipid peroxidation of rat liver homogenates *in vitro*. Moreover, the introduction of the  $-\text{CH}_2-$  spacer leads to a significant increase of antioxidant properties. It is also shown that compounds don't affect calcium-induced mitochondrial swelling and the mitochondrial membrane potential. No cytotoxicity was found for the compounds. Results of this study open the scopes for the search of novel water-soluble drugs with antioxidant properties.

## Acknowledgments

The financial support of RFBR № 18-03-00203, 19-33-90236, 20-03-00471 (synthesis, electrochemical and EPR studies), and RSF № 19-13-00084 (experiments on lipid peroxidation) is gratefully acknowledged. Studies of mitochondrial functions and influence on cell viability were supported by Russian State assignment № 0090-2019-0005. The EPR measurements were performed using spectrometer of MSU Chemistry Department "Nanochemistry and Nanomaterials" Equipment Center, supported by Moscow State University Program of Development. The equipment of Center for Collective Use IPAC RAS (agreement N14.621.21.0008, ID RFMEFI62114X0008) was used in the biological experiments.

## Conflicts of interest

We confirm that there are no known conflicts of interest associated with this publication.

## References

- Klaunig JE, Wang Z. Oxidative stress in carcinogenesis. *Curr Opin Toxicol*. 2018;7:116–121.
- Giustarini D, Dalle-Donne I, Tsikas D, et al. Oxidative Stress and Human Diseases: Origin, Link, Measurement, Mechanisms, and Biomarkers. *Critical Rev Clin Lab Sci*. 2009;46(5-6):241–281.
- Preedy VR. *Aging: Oxidative Stress and Dietary Antioxidants*. 1st ed. Academic Press; 2014. 301 p.
- Niki E. Oxidant-specific Biomarkers of Oxidative Stress. Association with Atherosclerosis and Implication for Antioxidant Effects. *Free Rad Biol Med*. 2018;120:425–440.
- Mahadik SP, Pillai A, Joshi S, et al. Prevention of oxidative stress-mediated neuropathology and improved clinical outcome by adjunctive use of a combination of antioxidants and omega-3 fatty acids in schizophrenia. *Int Rev Psych*. 2006;18:119–131.
- Gupta S, Agarwal A, Sharma RK. The Role of Placental Oxidative Stress and Lipid Peroxidation in Preeclampsia. *Obstet Gynecol Surv*. 2005;60(12):807–816.
- Patel M. Mitochondrial Dysfunction and Oxidative Stress: Cause and Consequence of Epileptic Seizures. *Free Rad Biol Med*. 2004;37(12):1951–1962.
- Rocha-Pereira P, Santos-Silva A, Rebelo I, et al. The Inflammatory Response in Mild and in Severe Psoriasis. *Br J Dermatol*. 2004;150(5):917–928.
- Klaunig JE, Wang Z. Oxidative stress in carcinogenesis. *Curr Opin Toxicol*. 2018;7:116–121.
- Desai A, Jain M, Ahuja R, et al. Role of antioxidants in cancer: a review. *Eur J Biomed Pharm Sci*. 2018;5(4):200–204.
- Liochev SI. Reactive Oxygen Species and the Free Radical Theory of Aging. *Free Rad Biol Med*. 2013;60:1–4.
- Pomatto LCD, Davies KJA. Adaptive Homeostasis and the Free Radical Theory of Ageing. *Free Rad Biol Med*. 2018;124:420–430.
- Ighodaro OM, Akinloye OA. First line defence antioxidants-superoxide dismutase (SOD), catalase (CAT) and glutathione peroxidase (GPX): Their fundamental role in the entire antioxidant defence grid. *Alexandria J Med*. 2018;54(4):287–293.
- Halliwel B. Antioxidants in Human Health and Disease. *Annu Rev Nutr*. 1996;16:33–50.
- Armstrong D. *Methods in molecular biology: oxidants and antioxidants: ultrastructure and molecular biology protocols*. Totowa: Humana Press Inc; 2002. 356 p.
- Denisov ET, Denisova G. *Handbook of Antioxidants: Bond Dissociation Energies, Rate Constants, Activation Energies and Enthalpies of Reactions*. CRC Press LLC; 2000. 190 p.
- Milaeva ER, Gerasimova OA, Jingwei Z, et al. Synthesis and antioxidative activity of metalloporphyrins bearing 2,6-di-tert-butylphenol pendants. *J Inorg Biochem*. 2008;102(5):1348–1358.
- Milaeva ER, Filimonova SI, Dubova LG, et al. Antioxidative Activity of Ferrocenes Bearing 2,6-Di-Tert-Butylphenol Moieties. *Bioinorg Chem Appl*. 2010;165482:1–6.
- Milaeva ER, Shpakovsky DB, Maklakova IA, et al. Novel diphenylsulfimide antioxidants containing 2,6-di-tert-butylphenol moieties. *Russ Chem Bull*. 2018;67(11):2025–2034.
- Milaeva ER, Shpakovsky DB, Meleshonkova NN, et al. Novel ferrocene-based inhibitor of proteins glycation. *Rus Chem Bull Int Ed*. 2015;64(9):2195–2202.
- Mikhalev OV, Shpakovsky DB, Gracheva Yu A, et al. Synthesis and study of new phenolic antioxidants with nitroaromatic and heterocyclic substituents. *Russ Chem Bull Int Ed*. 2018;67(4):712–720.
- Milaeva ER, Shpakovsky DB, Gracheva Yu A, et al. Metal complexes with functionalised 2,2'-dipicolylamine ligand containing an antioxidant 2,6-di-tert-butylphenol moiety: synthesis and biological studies. *Dalton Trans*. 2013;42(19):6817–6828.
- Shpakovsky DB, Shtil AA, Kharitonashvili EV, et al. The antioxidant 2,6-di-tert-butylphenol moiety attenuates the pro-oxidant properties of the auranofin analogue. *Metallomics*. 2018;10(3):406–413.
- Shpakovsky DB, Banti CN, Beaulieu-Houle G, et al. Synthesis, structural characterization and *in vitro* inhibitory studies against human breast cancer of the bis-(2,6-di-tert-butylphenol)tin(IV) dichloride and its complexes. *Dalton Trans*. 2012;41(48):14568–14582.
- Antonenko TA, Shpakovsky DB, Vorobyov MA, et al. Antioxidative vs cytotoxic activities of organotin complexes bearing 2,6-di-tert-butylphenol moieties. *Appl Organomet Chem*. 2018;32(7):e4381.
- Milaeva ER. Metal-Based Antioxidants - Potential Therapeutic Candidates for Prevention the Oxidative Stress - Related Carcinogenesis: Mini-Review. *Curr Top Med Chem*. 2011;11(21):2703–2713.
- Milaeva ER, Tyurin V Yu. Hybrid metal complexes with opposed biological modes of action – promising selective drug candidates. *Pure Appl Chem*. 2017;89(8):1065–1088.



28. Coffield H, Filbey AH, Ecke GG, et al. Some Reactions of 2,6-Dialkylphenols. *J Am Chem Soc.* 1957;79:5019–5023.
29. X-AREA, X-RED32, Stoe & Cie: Darmstadt, Germany; 2012.
30. Farrugia LJ. WinGX and ORTEP for Windows: an update. *J Appl Crystallogr.* 2012;45:849–854.
31. Sheldrick GM. A Short History of SHELX. *Acta Crystallogr Sect A: Fundam Crystallogr.* 2008;64(Pt 1):112–122.
32. Macrae CF, Edington PR, McCabe P, et al. Mercury: visualization and analysis of crystal structures. *J Appl Crystallogr.* 2006;39(3):453–457.
33. Tyurin V Yu, Meleshonkova NN, Dolganov AV, et al. Electrochemical method in determination of antioxidative activity using ferrocene derivatives as examples. *Russ Chem Bull Int Ed.* 2011;60(4):647–655.
34. Tyurin V Yu, Moiseeva AA, Shpakovsky DB, et al. The electrochemical approach to antioxidant activity assay of metal complexes with dipicolylamine ligand, containing 2,6-di-tert-butylphenol groups, based on electrochemical DPPH-test. *J Electroanal Chem.* 2015;756:212–221.
35. Brand-Williams W, Cuvelier M, Berset C. Use of a free radical method to evaluate antioxidant activity. *Food Sci Technol.* 1995;28(1):25–30.
36. Apak R, Guclu K, Ozyurek M, et al. Novel Total Antioxidant Capacity Index for Dietary Polyphenols and Vitamins C and E, Using Their Cupric Ion Reducing Capability in the Presence of Neocuproine: CUPRAC Method. *J Agric Food Chem.* 2004;52(26):7970–7981.
37. Kubo I, Masuoka N, Ha TJ, et al. Antioxidant activity of anacardic acids. *Food Chem.* 2006;99(3):555–562.
38. Xanthopoulou MN, Hadjikakou SK, Hadjiladis N, et al. Biological studies of new organotin(IV) complexes of thioamide ligands. *Eur J Med Chem.* 2008;43(2):327–335.
39. Erdahl WL, Krebsbach RJ, Pfeiffer DR. A comparison of phospholipid degradation by oxidation and hydrolysis during the mitochondrial permeability transition. *Arch Biochem Biophys.* 1991;285(2):252–260.
40. Whipps DE, Halestrap AP. Rat liver mitochondria prepared in mannitol media demonstrate increased mitochondrial volumes compared with mitochondria prepared in sucrose media. *Biochem J.* 1984;221:147–152.
41. Gornall AG, Bardawill CJ, David MM. Determination of Serum Proteins by Means of the Biuret Reaction. *J Biol Chem.* 1949;177(2):751–766.
42. Shevtzova EF, Kireeva EG, Bachurin SO. Effect of beta-Amyloid Peptide Fragment 25-35 on Nonselective Permeability of Mitochondria. *Bull Exp Biol Med.* 2001;132(6):1173–1176.
43. Niks M, Otto M. Towards an Optimized MTT Assay. *J Immunol Methods.* 1990;130(1):149–151.
44. Milaeva ER, Tyurin VYu, Shpakovsky DB, et al. Redox-active metal complexes with 2,2'-dipicolylamine containing ferrocenyl moiety: Synthesis, electrochemical behavior and biological activity. *J Organomet Chem.* 2017;839:60–70.
45. Strel'nikov AI, Tomilova IK, Safronova BG, et al. Comparative study of in vivo impact of water-soluble and lipophilic forms of dipicolylamine containing a 2,6-di-tert-butylphenol moiety on the oxidative status of rat tissues. *Russ Chem Bull Int Ed.* 2014;63(5):1238–1242.
46. Meleshonkova NN, Shpakovsky DB, Fionov AV, et al. Synthesis and redox properties of novel ferrocenes with redox active 2,6-di-tert-butylphenol fragments: The first example of 2,6-di-tert-butylphenoxy radicals in ferrocene system. *J Organomet Chem.* 2007;692(24):5339–5344.
47. Milaeva ER. Ligand oxidation as a method for intramolecular activation of metal complexes. *Russ Chem Bull.* 2001;50:573–586.
48. Salazar R, Navarrete-Encina PA, Squella JA, et al. Study on the oxidation of C4-phenolic-1,4-dihydropyridines and its reactivity towards superoxide radical anion in dimethylsulfoxide. *Electrochim Acta.* 2010;56(2):841–852.
49. He JB, Yuan SJ, Du JQ, et al. Voltammetric and spectral characterization of two flavonols for assay-dependent antioxidant capacity. *Bioelectrochem.* 2009;75(2):110–116.
50. Garrido EM, Lima JLFC, Delerue-Matos C, et al. Electrochemical oxidation of propanil and related N-substituted amides. *Anal Chim Acta.* 2001;434(1):35–41.
51. Salas-Reyes M, Hernández J, Domínguez Z, et al. Electrochemical Oxidation of Caffeic and Ferulic Acid Derivatives in Aprotic Medium. *J Braz Chem Soc.* 2011;22(4):693–701.
52. Sánchez A, Guillén-Villara RC, Sánchez R, et al. Electrochemical Oxidation of Symmetrical Amides of Ferulic Acid in Aprotic Medium. *Electrochim Acta.* 2014;133:546–554.
53. Lund H, Hammerich O. *Organic Electrochemistry*. New York: Marcel Dekker; 2001. 1393 p.
54. Elgrishi N, Rountree KJ, McCarthy BD, et al. A Practical Beginner's Guide to Cyclic Voltammetry. *J Chem Educ.* 2018;95(2):197–206.
55. Mann CK, Barnes KK. *Electrochemical Reactions in Nonaqueous Systems*. New York: Marcel Dekker; 1970. 560 p.
56. Tyurin V, Zhang J, Glukhova A, et al. *Macroheterocycl.* 2011;4:211–212.
57. Solon E, Bard AJ. The Electrochemistry of Diphenylpicrylhydrazyl. *J Am Chem Soc.* 1964;86(10):1926–1928.
58. Bondet V, Brand-Williams W, Berset C. Kinetics and Mechanisms of Antioxidant Activity using the DPPH.Free Radical Method. *Food Sci Technol.* 1997;30(6):609–615.
59. Andreou A, Feussner I. Lipoxygenases - Structure and Reaction Mechanism. *Phytochem.* 2009;70(13-14):1504–1510.
60. Nakano H, Inoue T, Kawasaki N, et al. Synthesis and Biological Activities of Novel Antiallergic Agents With 5-lipoxygenase Inhibiting Action. *Bioorg Med Chem.* 2000;8(2):373–380.
61. Pontiki E, Hadjipavlou-Litina D, Litinas K, et al. Design, Synthesis and Pharmacobiological Evaluation of Novel Acrylic Acid Derivatives Acting as Lipoxygenase and cyclooxygenase-1 Inhibitors With Antioxidant and Anti-Inflammatory Activities. *Eur J Med Chem.* 2011;46(1):191–200.
62. Werz O, Steinhilber D. Therapeutic Options for 5-lipoxygenase Inhibitors. *Pharmacol Therapeut.* 2006;112(3):701–718.
63. Erdahl WL, Krebsbach RJ, Pfeiffer DR. A Comparison of Phospholipid Degradation by Oxidation and Hydrolysis During the Mitochondrial Permeability Transition. *Arch Biochem Biophys.* 1991;285(2):252–260.
64. Fulda S, Galluzzi L, Kroemer G. Targeting Mitochondria for Cancer Therapy. *Nat Rev Drug Discov.* 2010;9(6):447–464.